NUCLEON FORM FACTORS USING SPIN DEGREES OF FREEDOM

M. K. JONES
Jefferson Lab
Newport News, Va, USA
E-mail: jones@jlab.org

An overview of recent measurements of the neutron and proton electromagnetic form factors from double polarization experiments. Spin observables are sensitive to the product of nucleon form factor which allows access to the small nucleon electric form factors.

1. Introduction

The nucleon form factors describe the internal structure of the nucleon. The elastic electron-nucleon reaction can be used to access the form factors. The earliest experiments in elastic electron-proton scattering established[1] the dominance of one-photon exchange and that the proton's Dirac, F_1, and Pauli, F_2, form factors depended only on Q^2, the four-momentum transfer squared. The proton and neutron are isospin partners, so their form factors are related. The unpolarized elastic electron-nucleon cross section, assuming one-photon exchange, is

$$\sigma = k\sigma_{Mott}\left[(F_1 - \kappa\tau F_2)^2 + \frac{\tau}{\epsilon}(F_1 + \kappa F_2)^2\right], \tag{1}$$

where k is a kinematic factor,σ_{Mott} is the Mott cross-section, $\epsilon = [1+2(1+\tau)\tan^2(\frac{\theta_e}{2})]^{-1}$ with θ_e being the electron scattering angle and $\tau = Q^2/4M^2$ in which M is the nucleon mass. One can define the electric, G_E, and magnetic, G_M, form factors as:

$$G_E = F_1 - \kappa\tau F_2 \text{ and } G_M = F_1 + \kappa F_2. \tag{2}$$

with κ being the anomalous magnetic moment. At $Q^2 = 0$, the electric and the magnetic form factors are the total charge and magnetic moment. G_{Ep} and G_{Mp} can be determined by measuring the cross-sections at a fixed Q^2 over a range of ϵ by varying the incident beam energy. The lack of a free

neutron target makes measuring the neutron form factors difficult. Cross-section measurements of inelastic electron-deuteron scattering have been used to measure the neutron form factors, but the extraction is sensitive to modeling of the deuteron wave function, final state interaction and meson exchange. In addition, since the net charge of the neutron is zero, neutron electric form factor is small. Therefore an experiment is needed in which the observable is a product of form factors.

The development of high current, high duty factor and highly polarized electron beams has made precision measurement of polarization observables in double polarization experiments feasible. The double polarization experiments use a polarized electron beam that is elastically scattered either on a polarized nucleon target in beam-target asymmetry measurement or from a unpolarized nucleon target and the transverse component of the scattered nucleon's polarization is measured. Both of these polarization observables are proportional[2,3] to $G_E G_M$. For a proton target, these double polarization experiments are relatively straight forward, but for the neutron one needs a nuclear target. It has been shown[4] that measurement of the outgoing neutron polarization in exclusive $^2\mathrm{H}(\vec{e}, e'\vec{n})$ at quasi-free kinematics would be sensitive to $G_E G_M$, but relatively insensitive to details of the reaction. For asymmetry measurements a polarized target is needed. Using ^{3}He as a effective neutron target was pointed out by Ref. 5 and 6, since, effectively, the protons pair to form a S-state and the neutron carries the entire spin of ^{3}He. Calculations[7,8] have shown that beam-target asymmetry measurements using a polarized ^{2}H or ^{3}He target and exclusive scattering at quasi-free kinematics allows the determination of G_{En} with minimal model dependence. The following sections will describe how the nucleon form factors have been measured in double polarization experiments.

2. Proton Electric Form Factor

At Q^2 below 1 GeV^2, G_{Ep} and G_{Mp} have been determined with small error bars and $\mu_p G_{Ep}/G_{Mp}$ was found to be ≈ 1. The measurements of $\mu \mathrm{G}_{Ep}/\mathrm{G}_{Mp}$ from cross section data are plotted in in Fig. 1 as open points. At $\mathrm{Q}^2 < 1$ GeV^2, the Vector Meson Dominance (VMD) model (see e.g. Ref. 9) has been successful in modeling the nucleon form factors which indicates the need for a pionic degree of freedom in a model of nucleon factors in this Q^2 region. As Q^2 increases, the elastic ep cross section is dominated by the G_{Mp} contribution. As indicated by the scatter of the $\mu \mathrm{G}_{Ep}/\mathrm{G}_{Mp}$ measurements above $\mathrm{Q}^2 > 2$ GeV^2 determination of G_{Ep} is

difficult from cross-section data. Conversely, G_{Mp} can be obtained from cross-section data with minimal error due to assumptions about G_{Ep}, so G_{Mp} is measured[10] up to $Q^2 = 31$ GeV^2.

Another approach to determining G_{Ep} is to measure the longitudinal, P_L, and transverse, P_T, polarization components of the outgoing proton in the $p(\vec{e}, e'\vec{p})$ elastic reaction. In terms of these polarization components and in the one-photon exchange approximation, the ratio of the electric to magnetic form factors can be written[3,4] as:

$$\frac{G_{Ep}}{G_{Mp}} = -\frac{P_T}{P_L}\frac{(E_e + E_{e'})}{2M}\tan(\frac{\theta_e}{2}). \tag{3}$$

in which $E_{e'}$ is the scattered electron's energy and E_e is the incident beam energy. The protons are detected in a magnetic spectrometer which bends the protons upward to the focal plane detectors. A polarimeter in the focal plane measures the transverse, P'_T, and normal, P'_N, components of the proton polarization. To extract the focal plane polarization components, one measures the number of protons which scattered from the analyzer as a function of their azimuthal scattering angle, φ, which can be expressed as:

$$N_p^{\pm}(\varphi) = N_p^{\circ\pm}\Big[1 \pm hA_y(P'_T \sin\varphi - P'_N \cos\varphi)\Big] \tag{4}$$

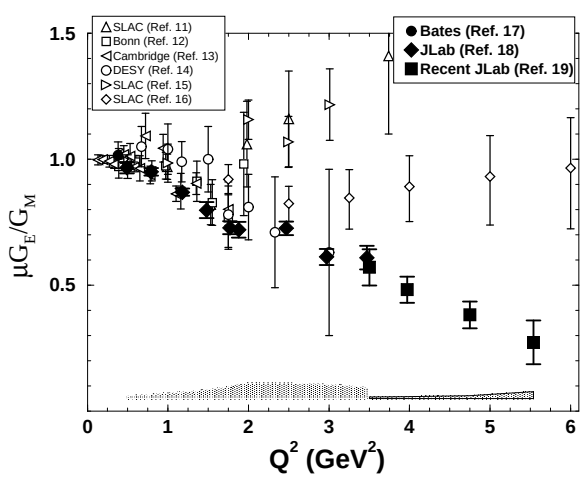

Figure 1. The open points are world data for $\mu_p G_{Ep}/G_{Mp}$ from cross section measurements. The filled points are $\mu_p G_{Ep}/G_{Mp}$ from polarization measurements.

A_y is the analyzing power polarimeter. $N_p^{\circ\pm}$ is the average number of scattered protons and the $\pm$ represents the beam helicity, h, aligned either parallel or anti-parallel to the beam momentum. In the case of a simple dipole magnet, the relation between the polarizations at the focal plane and those at the target is $P'_T = P_T$ and $P'_N = P_L \cdot sin\chi$ where χ is the spin precession angle. In general, the magnetic elements of the spectrometer are more complicated and a spin precession matrix has to be used to extract target polarizations from the focal plane polarizations. By taking the ratio of polarization components, the factors of analyzing power and beam helicity cancel and the systematic error is reduced.

An experiment[17] at MIT-Bates first used this method to determine G_{Ep}/G_{Mp} at $Q^2 = 0.38$ and 0.5 GeV^2 and the data is plotted as filled circles in Fig. 1. In 1998 at Thomas Jefferson National Laboratory (JLab), G_{Ep}/G_{Mp} was measured[18] for Q^2 between 0.5 to 3.5 GeV^2 in Hall A. The data are plotted as filled diamonds in Fig. 1. From this data, G_{Ep}/G_{Mp} has a linear fall-off as a function of Q^2. To find out if this linear trend continued, measurements of G_{Ep}/G_{Mp} at JLab were extended[19] to $Q^2 =$ 5.6 GeV^2 and the new data points are plotted at filled squares in Fig. 1. The overlap point at $Q^2 = 3.5$ GeV^2 agrees between the two experiments and the ratio continues to drop linearly. The systematic error for the JLab data are shown as filled in polygons at the bottom of Fig. 1. Understanding the total bend angle in the dispersive and non-dispersive planes of the spectrometer is the major source of systematic error in the JLab data. Careful study[20] the bend angle was done, and this reduced the systematic error by a factor of six compared to the first JLab experiment. A reanalysis of the systematic errors for the first JLab experiment is underway.

Instead of calculating G_{Ep}/G_{Mp}, Eq. 2 can be used to calculate F_2/F_1. In Fig. 2, the ratio QF_2/F_1 is plotted and the data from JLab are flat above $Q^2 = 1.8$ GeV^2. The weighted average of the QF_2/F_1 above $Q^2 =$ 1.8 GeV^2 is 0.70 (solid line in Fig. 2). Assuming hadron helicity conservation, the expectation[21] is that $Q^2F_2/F_1 \propto constant$ which is not meet in this Q^2 range. From the initial hint in the first JLab experiment, Ralston *et al.* had predicted that QF_2/F_1 would continue to be constant above $Q^2 =$ 3.5 GeV^2, because of nonzero angular momentum in the nucleon wavefunction. Ralston elaborates on this theory in a contribution to this Workshop. Miller and Frank demonstrated[23] that in a relativistic constituent quark model and imposing Poincare invariance leads to a violation of hadron helicity conservation and the prediction that $QF_2/F_1 \propto constant$ in this Q^2 range.

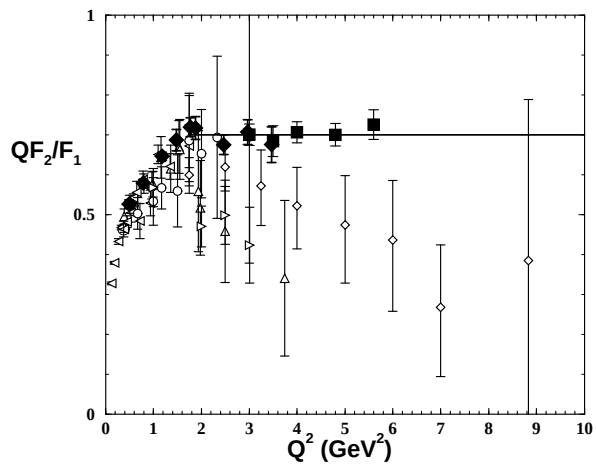

Figure 2. The open (filled) points are world data for QF_2/F_1 from cross-section (polarizations) measurements. Symbols same as Fig. 1.

3. Neutron Magnetic Form Factor

The neutron magnetic form factor, G_{Mn}, can be extracted from cross-section measurement of the $^2H(e,e')$ inelastic reaction at quasi-free kinematics. The cross-section can be written as:

$$\sigma = k\sigma_{Mott}\{R_L + \epsilon R_T\} \tag{5}$$

in which R_L and R_T are the longitudinal and transverse response functions which depend on Q^2 and the energy transfer. By measuring cross sections at different ϵ, R_L and R_T are determined. In the plane wave impulse approximation (PWIA), $R_L \propto G_{Ep}^2 + G_{En}^2$ and $R_T \propto G_{Mp}^2 + G_{Mn}^2$. Therefore both G_{Mn} and G_{En} can be extracted using previous measurements of the proton form factors, though sensitivity to the deuteron wave function, final state interactions (FSI) and meson exchange currents (MEC) limits the accuracy in determining G_{Mn}.

To avoid subtraction of the proton contribution to the inclusive inelastic cross section, one can measure $^2H(e,e'n)$ reaction at quasi-free kinematics. This measurement was done at MIT-Bates[24] at $Q^2 = 0.108$, 0.176 and 0.255. The extracted G_{Mn} plotted as open triangles in Fig. 3. The major difficulty with these coincidence measurements is that absolute knowledge of the neutron detection efficiency is needed for the cross-section measurement. In addition, the exclusive reaction still has a sensitivity to the deuteron wave function, FSI and MEC. This sensitivity can minimized by measuring

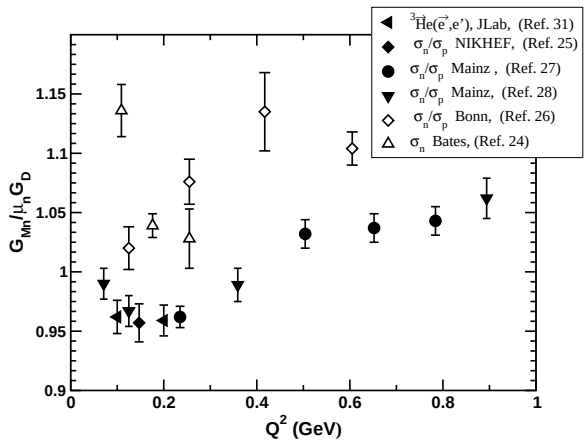

Figure 3. Recent measurements of $G_{Mn}/\mu_n G_D$. $G_D = 1/(1+Q^2/.71)^2$

the ratio of the cross-sections, σ_n/σ_p, for ^{2}H$(e,e'n)$ to ^{2}H$(e,e'p)$ reactions. In Fig. 3, measurements of G$_{Mn}$ using the ratio technique are shown from experiments done at NIKHEF[25] (filled diamond), Bonn[26] (open diamonds) and at Mainz Microtron (MAMI)[27,28] (filled upside-down triangles[27] and filled circles[28]). The experiments use different methods for determining the neutron detection efficiency, and a systematic difference in values of G$_{Mn}$ can be seen.

Using polarization observables to measure G$_{Mn}$ is an attractive alternative to the cross-section measurement, since the systematic errors will be different. The beam-target asymmetry, A, for the inclusive $^3\vec{\text{He}}(\vec{e},e')$ at quasi-free kinematics has been shown[8] to have a sensitivity to G$_{Mn}$ and a relative insensitivity to other aspects of the model. The beam-target asymmetry can be written[29] as:

$$A = \frac{-(\nu_{T'} R_{T'} \cos\Theta + 2\sin\Theta\cos\phi\nu_{LT'} R_{LT'})}{R_L + \epsilon R_T} \tag{6}$$

in which the ν_i are kinematic factors and $R_{T'}$ and $R_{LT'}$ are the spin-dependent transverse and longitudinal-transverse response functions. Θ and ϕ are the angles of the target spin relative to the 3-momentum transfer vector. By orienting target polarization is along the q-vector, one measures the asymmetry, $A_{T'}$, which is proportional to $R_{T'}$. In the PWIA, $R_{T'}$ is proportional to G$^2_{Mn}$. The first experiment was done a MIT-Bates [30]. Recently at JLab, $A_{T'}$ was measured for $^3\vec{\text{He}}(\vec{e},e')$ at quasielastic kinematics for Q^2 = 0.1 to 0.6 in steps of 0.1 GeV^2. To extract G$_{Mn}$, at a precision

comparable to the determination done with cross-section ratios, a model of the $^3\vec{\mathrm{He}}(\vec{e}, e')$ reaction is needed. Golak et al. [8] did a full non-relativistic Faddeev calculations with realistic NN forces including meson exchange currents. At $Q^2 = 0.1$ and 0.2 GeV^2, calculations of $A_{T'}$ as a function of the energy transfer were done. G_{Mn} is extracted be varying G_{Mn} within the model and finding the best agreement with the data. The results for G_{Mn} are plotted as filled right triangles in Fig. 3 and agree with the G_{Mn} from MAMI [27,28] and NIKHEF[25].

4. Neutron Electric Form Factor

Elastic *ed* cross section measurements have been used to extract G_{En}. In the early 70's, Galster *et al.* extracted [32] G_{En} from *ed* elastic scattering cross section measurements for Q^2 up to 0.78 GeV^2, but the extraction is sensitive to the contribution from the proton electric form factor, the model of the deuteron wave function, FSI, and MEC. Nearly two decades later, more precise cross-section measurements [33] were done by Platchkov *et al.*. The dominant uncertainty in extracting G_{En} was which nucleon-nucleon potential to use. This gave about a factor of 2 uncertainty in the extracted value of G_{En}.

At Jefferson Lab, the tensor polarization observables of the scattered deuteron in *ed* elastic scattering were measured[34]. Schiavilla and Sick[35] combined the Jefferson Lab data with previous cross-section measurements to extract the deuteron's charge, magnetic and quadrupole form factors. They showed that different theoretical calculations of quadrupole form factor are in relatively close agreement to each other when compared to their sensitivity to the value of G_{En} used in the calculation. Their values for G_{En} are plotted as open diamonds in Fig. 4, and the error bar includes the experimental error and an error for the model dependence.

Another approach to measuring G_{En} is by double polarization experiments using a polarized electron beam with either polarized targets or measure the polarization of the scattered neutron. By detecting the neutron in coincidence with the electron, one can select quasi-free kinematics, so the effect of the proton in deuteron is minimized. In beam-target asymmetry measurements, the target can be either polarized deuterium or ^{3}He. For a free neutron, the beam-target asymmetry, A, is related to the form factors as[5,29]:

$$A = P_e P_N V \{ \frac{a G_{En} G_{Mn} \sin\Theta \cos\phi + b G_{Mn}^2 \cos\Theta}{G_{En}^2 + \frac{\tau}{\epsilon} G_{Mn}^2} \}. \tag{7}$$

P_e is the beam helicity. P_N is the neutron polarization. V is a dilution factor. a and b are kinematic factors, and Θ and ϕ describe the direction of the neutron's spin relative to the momentum transfer. The spin of the $^3\vec{He}$ can be oriented at $\Theta = 0°(90°)$, so the neutron's spin is parallel (perpendicular) to the momentum transfer vector.

Asymmetry measurements, $A_\parallel$ ($A_\perp$), are done for the $^3\vec{He}(\vec{e}, e'n)$ reaction for the spin of the $^3\vec{He}$ oriented parallel (perpendicular) to the momentum-transfer vector. Since G_{En} is much smaller than G_{Mn}, $A_\parallel$ is insensitive to the form factors. $A_\perp$ is sensitive to the ratio G_{En}/G_{Mn}. Therefore, the ratio of the neutron form factors is:

$$\frac{G_{En}}{G_{Mn}} \propto \frac{A_\perp}{A_\parallel} \tag{8}$$

and the sensitivity to the absolute value of the target and beam polarizations is eliminated and the dilution factor, V, cancels. At MAMI, measurements of $A_\parallel$ and $A_\perp$ have been done for the $^3\vec{He}(\vec{e}, e'n)$ reaction at $Q^2 = 0.4$ GeV^2 by the A3 collaboration [37] and at $Q^2 = 0.67$ GeV^2 by the A1 collaboration [38]. To extract G_{En} from the $^3\vec{He}(\vec{e}, e'n)$ asymmetry data, one needs a model of the $^3\vec{He}(\vec{e}, e'n)$ reaction. The same model [8], described above for extracting G_{Mn} from inclusive $^3\vec{He}(\vec{e}, e')$ asymmetry measurements, was used to extract G_{En} for the $Q^2 = 0.4$ GeV^2 with the exception that for this exclusive reaction meson exchange currents were not included. The calculations[8] of $\frac{A_\perp}{A_\parallel}$ indicate the importance of final state interactions as a function of outgoing neutron momentum, but at the kinematics of the experiment the difference between PWIA and the full calculation was about 10%. In Fig. 4, the results for G_{En} extracted using the model of Ref. 8 are plotted as filled diamonds. G_{En} was extracted from the $\frac{A_\perp}{A_\parallel}$ measurement at $Q^2 = 0.67$ by the A1 collaboration[38] without corrections for FSI and the value is plotted in Fig. 4 as a filled upside-down triangle.

Another option is to use a deuterium as a neutron target. Experiments have measured beam-target asymmetry of the $^2\vec{\mathrm{H}}(\vec{e}, e', n)$ reaction at quasi-free kinematics. At NIKHEF, asymmetry measurements were done using an internal polarized deuterium gas target. While at JLab, a dynamically polarized solid deuterated ammonia target was used[40]. Because of the large acceptance of the detectors needed to obtain good statistics in a reasonable amount of beam time, one has to account for the change of the asymmetry within the acceptance due to kinematical factors. In addition, the effects of FSI and MEC corrections may change with the kinematics within the

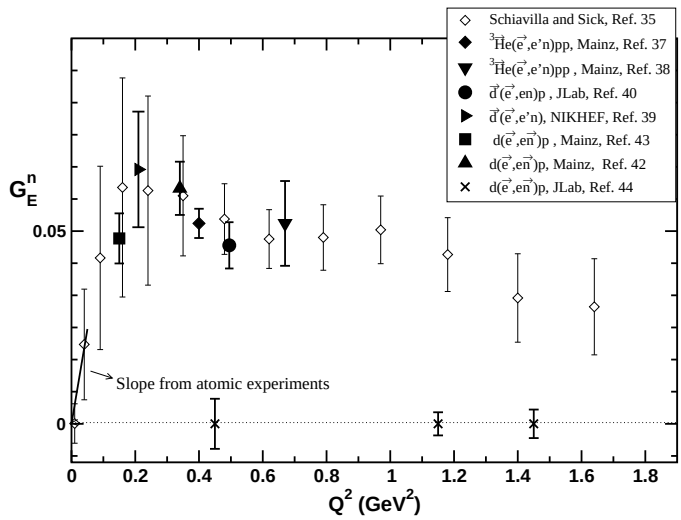

Figure 4. Filled points are world data for G_{En} from double polarization experiments. The open diamonds are for G_{En} from analysis of Schiavilla and Sick[35]. The solid line is the slope for G_{En} from the neutron charge radius measured in atomic collision experiment[36]. The points marked by a cross are the projected error bars for G_{En} measured in a recent experiment at JLab[44].

acceptance. Both experiments used the model [7] of Arenhovel *et al.* in a Monte Carlo of the experiment to extract G_{En}. The data was binned as a function of different kinematic variables (such as missing momentum). Within the experimental acceptance, the theoretical prediction scaled with the value of G_{En}. G_{En} was determined by the best fit to the asymmetry data. The data point from NIKHEF at $Q^2 = 0.21$ GeV^2 is plotted as a filled left triangle in Fig. 4, while G_{En} at $Q^2 = 0.5$ GeV^2 from JLab is plotted as a filled circle. In Fall 2001, more data was taken at JLab at $Q^2 = 0.5$ and 1.0 GeV^2.

Instead of using a polarized deuterium target, one can study the reaction $^2H(\vec{e}, e', \vec{n})$ and measure the transverse,P_T , and longitudinal,P_L , components of the outgoing neutron's polarization. As shown in Eq. 3, the ratio of P_T/P_L is proportional to G_{En}/G_{Mn} for a free nucleon. The first measurement of P_T/P_L in $d(\vec{e}, e'\vec{n})$ at quasifree kinematics was at MIT-Bates[41]. Since that time, experiments have done at MAMI[42,43] at $Q^2 = 0.12$ and 0.34 GeV^2 and at JLab[44] for $Q^2 = 0.45$, 1.15 and 1.47 GeV^2.

Though the details of the experiment differ, the basic principles of $d(\vec{e}, e'\vec{n})$ experiments are similar. At MAMI, the electrons were detected in

a lead glass calorimeter, while at JLab the High Momentum Spectrometer (HMS) in Hall C was used. In both experiments, an array of scintillators detected the scattered neutron. In addition, this array also served as the analyzer of the polarimeter. The last part of the polarimeter is a second set of scintillator arrays which detect the secondary protons or neutrons from the scattering in the analyzer. The transverse component of the neutron's polarization , P'_T, at the analyzer is measured by the asymmetry of the number of neutrons which scatter up to the number which scatter down after interacting in the analyzer. The polarimeter can only measure the components of the neutron spin which are transverse to the neutron's momentum direction. Therefore to measure P_L, a magnet is placed between the target and the analyzer with the magnet's field perpendicular to the neutron's momentum. The neutron's spin will precess in the magnet field by an angle, χ, which is related to the strength of the magnetic field. The relationship between P'_T and the neutron polarization at the target is:

$$P'_T = P_e A_y (P_T \cos\chi + P_L \sin\chi) = A_\circ \sin(\chi + \chi_\circ) \tag{9}$$

in which $\chi_\circ$ is the phase shift, define as $\tan\chi_\circ = \frac{P_T}{P_L}$. By measuring P'_T at various precession angles, $\chi_\circ$ can be determined independently of beam helicity, P_e, and the analyzing power, A_y.

For the $Q^2 = 0.12$ GeV^2 measurement, the major correction for extracting the free $G_{En}/\ G_{Mn}$ from the measured P_T/P_L is the charge exchange of the outgoing proton into a neutron via pion exchange. The transverse polarization of the neutron from charge exchange has the opposite sign compared to the neutron which is directly knocked-out, since the signs of the proton and neutron magnetic moments are the opposite. This effectively reduces the measured P_T of the neutron from $d(\vec{e}, e'\vec{n})$ reaction. To extract P_T for the free neutron one has to correct for this effect. Because of the large acceptance of the detector, the change of kinematics within the detector acceptance has to be taken into account. Using a Monte Carlo which included the model of Arenhovel *et al.*, the difference between the full and the PWIA calculation was found and a correction to the measured P_T/P_L to give the value of P_T/P_L for the free neutron was determined. At $Q^2 = 0.12$ GeV^2, there was a 68% correction, but at $Q^2 = 0.34$ GeV^2 the correction was only 8%.

In Fig. 4, G_{En} values (from Ref. 43 in which corrections for FSI were included) from MAMI at $Q^2 = 0.12$ and 0.34 GeV^2 are plotted as a filled square and filled triangle, respectively. The major systematic for the MAMI data is from the kinematic reconstruction of events and the contribution of

non-quasifree events. In Fig. 4, the projected statistical error bars of G_{En} at $Q^2 = 0.45$, 1.15 and 1.47 GeV^2 are plotted as crosses for the recently completed JLab experiment. Since a spectrometer was used to detect electrons in the JLab experiment, the systematics due to kinematics and the contribution of non-quasifree events will be much smaller. The systematic errors are expected to be smaller than the statistical error bars.

5. Conclusion

Double polarization experiments have proved valuable in measuring nucleon form factors. Precise measurement of G_{Ep}/G_{Mp} by the ratio polarization components in the $p(\vec{e}, e'\vec{p})$ elastic reaction has been preformed up to $Q^2 = 5.6$ GeV^2 and are planned to be extended[45] to $Q^2 = 9$ GeV^2 in Hall C at JLab. The use of deuterium and ^{3}He as effective neutron targets has allowed access to the small neutron electric form factor. With different targets and polarization observables used to extract G_{En} the influence of different models of the target wavefunction and reaction mechanisms can be studied. As presented at the Workshop, an experiment in Hall A at JLab has been approved[46] to extract G_{En} to $Q^2 = 3.4$ GeV^2 by measuring the ratio of asymmetries in the $^3\vec{He}(\vec{e}, e'n)$ reaction. With precise measurement of all four nucleon electro-magnetic form factors understanding the structure of the nucleon is coming closer.

Acknowledgments

The Southern Universities Research Association (SURA) operates the Thomas Jefferson National Accelerator Facility for the United States Department of Energy under contract DE-AC05-84ER40150.

References

1. E.E. Chambers and R. Hofstadter, Phys. Rev. **103**, 1454 (1956).
2. N. Dombey, Rev. of Mod. Phys. **41**, 236 (1969).
3. A.I. Akhiezer and M.P. Rekalo, Sov. J. Part. Nucl. **3**, 277 (1974).
4. R. Arnold, C. Carlson and F. Gross, Phys. Rev. C **23**, 363 (1981).
5. B. Blankleider and R. M. Woloshyn, Phys. Rev. C **29**, 538 (1984).
6. J.L. Friar *et al.* , Phys. Rev. C **42**, 2310 (1990).
7. H. Arenhovel, W Leidemann, and E. L. Tomusiak, Phys. Rev. C **46**, 455 (1992). H. Arenhovel, W Leidemann, and E. L. Tomusiak, Z. Phys. A **331**, 123 (1988); **334**, 363(E) (1989).
8. J. Golak, G. Ziemer, H. Kamada, H. Witala and W. Glockle, Phys. Rev. C **63**, 034006 (2001). S. Ishikawa, J. Golak, H. Witala, H. Kamada, W. Glockle and D. Huber, Phys. Rev. C **57**, 39 (1998).

9. P. Mergell, U.G. Meissner, D. Drechsler Nucl. Phys. B **A596**, 367 (1996) ; and A.W. Hammer, U.G. Meissner and D. Drechsel, Phys. Lett. B **385**, 343 (1996).
10. A.F. Sill *et al.*, Phys. Rev. D **48**, 29 (1993).
11. J. Litt *et al.*, Phys. Lett. B **31**, 40 (1970).
12. Ch. Berger *et al.*, Phys. Lett. B **35**, 87 (1971).
13. L.E. Price *et al.*, Phys. Rev. D **4**, 45 (1971).
14. W. Bartel *et al.*, Nuc. Phys. B **58**, 429 (1973).
15. R.C. Walker *et al.*, Phys. Rev. D **49**, 5671 (1994).
16. L. Andivahis *et al.*, Phys. Rev. D **50**, 5491 (1994).
17. B. Milbrath *et al.*, Phys. Rev. Lett. **80**, 452 (1998).
18. M. K. Jones *et al.*, Phys. Rev. Lett. **84**, 1398 (2000).
19. O. Gayou *et al.*, Phys. Rev. Lett. **88**, 092301 (2002).
20. L. Pentchev *et al.*, JLab Technical Note No. TN-01-052, 2001.
21. S.J. Brodsky and G.P. Lepage, Phys. Rev. D24, 2848 (1981).
22. J. Ralston *et al.*, in *Intersections between Particle and Nuclear Physics*, AIP Conf. Proc. No. 509, 302 (AIP, Melville, NY 2000), hep-ph/0206074.
23. G. A. Miller and M. R. Frank, Phys. Rev. C65, 065205 (2002).
24. P. Markowitz *et al.*, Phys. Rev. C **48**, R5 (1993).
25. H. Anklin *et al.*, Phys. Lett. **B336** , 313 (1994).
26. E. E. W. Bruins *et al.*, Phys. Rev. Lett. **75** , 21 (1995).
27. H. Anklin *et al.*, Phys. Lett. **B428** , 248 (1998).
28. G. Kubon *et al.*, Phys. Lett. **B524** , 26 (2002).
29. T. W. Donnelly and A. S. Raskin, Ann. Phys. **169**, 247 (1986).
30. H. Gao *et al.*, Phys. Rev. C **50**, R546 (1994); H. Gao *et al.*, Nucl. Phys. **A631**, 170 (1998).
31. W. Xu *et al.*, Phys. Rev. Lett. **85**, 2900 (2000).
32. S. Galster, H. Klein, J. Moritz, K.H. Schmidt, D. Wegener, Nucl. Phys. **B32**, 221 (1971).
33. S. Platchkov *et al.*, Nucl. Phys. **A510**, 740 (1990).
34. D. Abbott *et al.*, Phys. Rev. Lett. **84**, 5053 (2000).
35. R. Schiavilla and I. Sick, Phys. Rev. C **64**, 041002 (2001).
36. S. Kopecky *et al.* , Phys. Rev. C **57**, 2229 (1997).
37. J. Becker *et al.*, Eur. Phys. J. A **6**, 329 (1999).
38. D. Rohe *et al.*, Phys. Rev. Lett. **83**, 4257 (1999).
39. I. Passchier *et al.*, Phys. Rev. Lett. **82**, 4988 (1999).
40. H. Zhu *et al.*, Phys. Rev. Lett. **87**, 081801 (2001).
41. T. Eden *et al.*, Phys. Rev. C **50**, R1749 (1994).
42. M. Ostrick *et al.*, Phys. Rev. Lett. **83**, 276 (1999).
43. C. Herberg *et al.*, Eur. Phys. J. A **5**, 131 (1999).
44. R. Madey *et al.* (The e93038 Collaboration), to be published in the Proceedings of the Baryons 2002 Conference.
45. TJNAF proposal E01-109, C. F. Perdrisat, V. Punjabi, E. Brash and M. K. Jones, spokepersons.
46. TJNAF proposal E02-013, B. Reitz, B. Wojtsekhowski, K. McCormick, G. Cates, spokepersons.